Journal of Molecular Catalysis A: Chemical 318 (2010) 51–59

Contents lists available at ScienceDirect

Journal of Molecular Catalysis A: Chemical

journal homepage: www.elsevier.com/locate/molcata

Structure and catalytic properties of MgO-supported vanadium oxide in the selective oxidation of cyclohexane

Eman Fahmy Aboelfetoh[a,b], Michael Fechtelkord[c], Rudolf Pietschnig[a,*]

[a] Karl-Franzens-Universität, Institut für Chemie, Schubertstraße 1, A-8010 Graz, Austria
[b] Chemistry Department, Faculty of Science, Tanta University, Tanta 31527, Egypt
[c] Institut für Geologie, Mineralogie und Geophysik, Ruhr-Universität Bochum, Universitätsstr. 150, D-44780 Bochum, Germany

ARTICLE INFO

Article history:
Received 13 August 2009
Received in revised form 9 November 2009
Accepted 11 November 2009
Available online 17 November 2009

Keywords:
C–H activation
Vanadium
Supported catalyst
MgO
Cyclohexane oxidation

ABSTRACT

MgO-supported vanadium oxide catalysts with different vanadium loadings have been prepared by wet impregnation and grafting using ammonium metavanadate or $VOCl_3$ as precursor, respectively. The prepared catalysts have been characterized by several techniques such as XRD, FT-IR, DR-spectroscopy, BET, ^{51}V solid-state NMR, SEM and EDX. For comparison, three different phases of magnesium vanadate (meta-β-MgV_2O_6, pyro-α-$Mg_2V_2O_7$, and ortho-$Mg_3V_2O_8$) have been synthesized as reference materials for the structural characterization. The catalytic activity of the prepared catalysts was evaluated for the liquid-phase oxidation of cyclohexane as a model reaction to obtain cyclohexylhydroperoxide, cyclohexanol and cyclohexanone with PCA as co-catalyst. The results show that VO_x/MgO catalysts containing isolated VO_4 species either impregnated or grafted do not show considerable activity in the oxidation process. In contrary, catalysts with higher vanadium loading, which contain ortho-$Mg_3V_2O_8$, pyro-$Mg_2V_2O_7$ and V_2O_5 phases as surface species show conversions up to 70% and TONs up to 34,700. Compared to previously studied support materials for this catalytic system the leaching behavior is significantly improved.

1. Introduction

Supported vanadium oxide catalysts have been reported extensively in the literature, because of their potential for catalyzing several oxidation reactions [1–11]. Especially the oxidation of lighter alkanes is promising with respect to alternative feedstocks for industrially relevant bulk chemicals [12–15]. The molecular structure of the supported vanadium oxide species was found to depend on several parameters, e.g., metal oxide loading, support oxide material, and degree of hydration [16–20]. The nature of the vanadium oxide species on several supports, i.e., Al_2O_3, Nb_2O_5, SiO_2, TiO_2, and ZrO_2, has been examined with several techniques [16,17,21–27]. Also the co-catalyst pyrazine 2-carboxylic acid (PCA) has a significant influence on the conversion of hydrocarbons. It is anticipated that PCA coordinates to vanadium sites on the catalyst surface facilitating electron and proton transfer processes between peroxo/hydroxyl species and vanadium [24,28,29].

Recently we studied Al_2O_3, TiO_2 and SiO_2 supported vanadium based catalysts for C–H activation of cyclohexane [24]. Obviously, the catalytic activity in various oxidation reactions over transition metal oxide catalysts changes with the support material [1,2,6]. In the course of our investigations it occurred to us that the basicity of the support material has a substantial influence on the catalytic performance and moreover on the leaching rate which can be a substantial problem for supported vanadium oxide catalysts. These findings prompted us to consider rather basic support materials like MgO as support materials for vanadium oxide species, which to our knowledge have not been used for this purpose so far.

Herein, we describe the preparation and structural characterization of MgO-supported V(V) catalyst as well as their catalytic performance in the partial oxidation of cyclohexane.

2. Experimental

Two different methods, grafting and wet impregnation, were applied to prepare supported vanadium oxide catalysts on MgO with different vanadium loadings following previously reported procedures [24]. For comparison magnesium meta-, pyro-, and ortho-vanadates (MgV_2O_6, $Mg_2V_2O_7$, and $Mg_3V_2O_8$, respectively) were prepared from $Mg(OH)_2$ and NH_4VO_3 according to the published methods [30,31], except the calcination conditions. The calcination conditions were as follows: 517 °C for 6 h and 629 °C for 6 h to MgV_2O_6; 550 °C for 6 h and 650 °C for 6 h to $Mg_2V_2O_7$; 550 °C for 21 h, 640 °C for 35 h and 675 °C for 60 h to $Mg_3V_2O_8$.

The catalytic activity of the prepared catalysts was evaluated for the liquid-phase oxidation of cyclohexane. The oxidation of

* Corresponding author. Tel.: +43 316 380 5287/5285; fax: +43 316 380 9835.
E-mail address: rudolf.pietschnig@uni-graz.at (R. Pietschnig).

1381-1169/$ – see front matter © 2009 Elsevier B.V. All rights reserved.
doi:10.1016/j.molcata.2009.11.007

cyclohexane (1.06 M, 27.56 mmol) was carried out in the presence of PCA (co-catalyst, 1.7×10^{-3} M, 0.044 mmol) at 60 °C for 24 h under atmospheric pressure in air using different weights of the catalyst with 30% aqueous H_2O_2 (oxidant, 0.4 M, 10.5 mmol) and 20 mL of solvent (acetonitrile). Molecular dioxygen acts as co-oxidant in agreement with the suggested mechanism for this model reaction [24,29]. The exact concentration of H_2O_2 is determined before the oxidation reaction by the permanganate method [32]. After the reaction, the catalyst was separated by centrifugation and the products are identified by GC–MS and their relative amounts are determined directly by its GC peak area using HP 6890 gas chromatography equipped with a split inlet (250 °C, split ratio 50.0) using HP 5 MS capillary column (30 m, 0.25 mm ID; constant flow of carrier gas helium 1.0 mL/min) coupled to a FID. The catalytic activities are reported as conversion (%), selectivity (%) and TON calculated following a published procedure [24]. The overall selectivity (OS%) is defined as sum of the selectivities for cyclohexylhydroperoxide, cyclohexanol and cyclohexanone.

The vanadium concentration of the prepared catalysts was determined by flame atomic absorption spectroscopy (AAS) using a UNICAM 929 AA spectrometer. The BET surface area of the catalysts was measured by nitrogen adsorption–desorption at 77 K using a NOVA 1200 surface area analyzer (Quanta-chrome). The isotherms were analyzed in a conventional manner in the region of the relative pressure, $p/p_0 = 0.05$–0.3. X-ray diffraction (XRD) patterns of all catalysts were performed on a Philips powder diffractometer PW1050/25 with Cu Kα radiation ($\lambda = 0.1542$ nm) operating at 50 kV and 20 mA in a 2θ range of 10–70° with step size 0.01° and time step 1.0 s to assess the crystallinity of the vanadium oxide loading. The diffractograms of the samples were compared with the powder diffraction patterns of reference samples. Fourier transform-infrared spectra of the samples were recorded on a Perkin-Elmer FT-IR spectrometer 1725x using KBr disks. Diffuse reflectance (DR) spectra in the UV–visible region were recorded in the reflectance function mode (F(R)) at room temperature in the range 1000–200 nm on a Varian Cary 500 spectrophotometer with a diffuse reflectance attachment to investigate the structures of $V(V^{5+})$-containing oxide compounds using MgO as a reference. Thermogravimetric analyses on both support material and all prepared catalysts were performed using a Mettler TGA. To evaluate the overall amount of surface hydroxyl groups available for anchoring reactions, the weight loss between 300 and 1000 °C was determined. A heating rate of 10 °C/min under argon was applied to purge off-gases from the TGA electronics and sample region. The reference material was α-alumina powder. The SEM analyses were done with a DSM 982 Gemini SEM with a maximum acceleration voltage of the primary electrons between 10 and 15 kV. The powder samples were prepared on double side adhesive carbon tape and covered with a gold layer in a Cressington sputter coater operated under vacuum conditions (0.5×10^{-1} mbar). Semi-quantitative EDX (Röntec, M-series, EDR288/SPU2) analysis was used for the characterization of element concentration and vanadium distribution within all prepared catalysts. The TEM examination of samples was carried out on a Philips CM10 microscope working at 100 kV. TEM specimens were prepared ultrasonically by dispersing the catalyst sample in ethanol, and then placing a drop of the suspension on a Cu grid covered with a lacey carbon film.[51] V-MAS-NMR spectra have been recorded on a Bruker ASX 400 WB at 105.152 MHz using a 4 mm HP WB 73 A MAS 4BL CPBB VTN probe at room temperature. Samples are measured in Y stabilized ZrO_2 rotors (4 mm) at spinning rate 12.5 kHz. The acquired data have been processed and analyzed using the program dmfit [33]. Further details and figures are available in electronic supporting information (ESI).

3. Results and discussion

3.1. Catalyst characterization

The vanadium content of the catalysts has been determined with AAS and EDX. Generally, the catalysts prepared by impregnation show higher vanadium contents than those prepared by grafting (Table 1). For comparison also an uncalcined grafted sample (Ungrf1Mg) is quoted, which is significantly hydrated as the increase of the vanadium content (by weight) upon calcination indicates.

For the impregnated catalysts a significantly lower vanadium concentration is obtained by EDX measurements compared to those determined by AAS. This discrepancy may be due to partial incorporation of vanadium in the bulk of the impregnated catalysts. The same trend is found for the grafted catalysts but to a much lower extent. The reason for this incorporation of vanadium could be consequence of the sheet-like morphology of MgO as found by SEM.

According to SEM, the MgO morphology consists of bundles of folded sheet-like crystals (Fig. 1A). At high vanadium loadings the impregnated catalysts show different phases besides aggregates of flake crystals of MgO. In the case of Imp4Mg smaller sized aggregates are observed (Fig. 1B), which is characteristic for ortho-$Mg_3V_2O_8$. By further increasing the loading (Imp5Mg), the aggregate-like structure becomes dominant and the size of the aggregates increases (Fig. 1C). This corresponds to the presence of pyro-$Mg_2V_2O_7$ at high V loading as confirmed from the surface composition analysis with EDX and SEM controlled with a reference sample. Catalyst Imp6Mg with the highest loading shows two different phases, one similar to that reported for pyro-$Mg_2V_2O_7$ and the other similar to V_2O_5 (Fig. 1D). These results are also confirmed by XRD and IR (see below).

3.1.1. Vanadium coverage

It has been previously shown that TGA can be used as a simple technique to determine the relative amount of surface hydroxyl

Table 1
Characteristics of MgO-supported vanadium oxide (VO_x/MgO) catalysts.

Catalyst	Color	V content (mmol/g catal.)	OH groups (mmol/g catal.)	Surface area (m^2/g MgO)	Pore volume cm^3/g catalyst	EDX V (wt.%)	AAS V (wt.%)
MgO	White	0.00	01.10	83.85	0.076	00.00	00.00
Ungrf1Mg	Dirty white	0.78	17.44	74.67	0.059	00.70 ± 00.29	03.97
Grf1Mg	Light yellow	1.08	02.32	223.27	0.174	03.42 ± 00.46	05.50
Grf2Mg	Yellow	2.62	02.14	–	–	06.58 ± 01.29	13.34
Grf3Mg	Yellow	3.32	01.93	133.82	0.094	10.61 ± 02.22	16.91
Imp1Mg	White	0.20	02.61	187.01	0.172	00.32 ± 00.12	01.02
Imp2Mg	Light yellow	1.08	02.41	–	–	01.08 ± 00.48	05.50
Imp3Mg	Light yellow	3.32	02.10	156.52	0.118	06.70 ± 04.40	16.91
Imp4Mg	Light yellow	4.53	01.96	–	–	14.00 ± 06.47	23.07
Imp5Mg	Brownish white	6.54	01.19	148.50	0.084	18.17 ± 11.98	33.31
Imp6Mg	Yellowish orange	9.81	00.83	109.50	0.045	31.14 ± 10.22	49.97

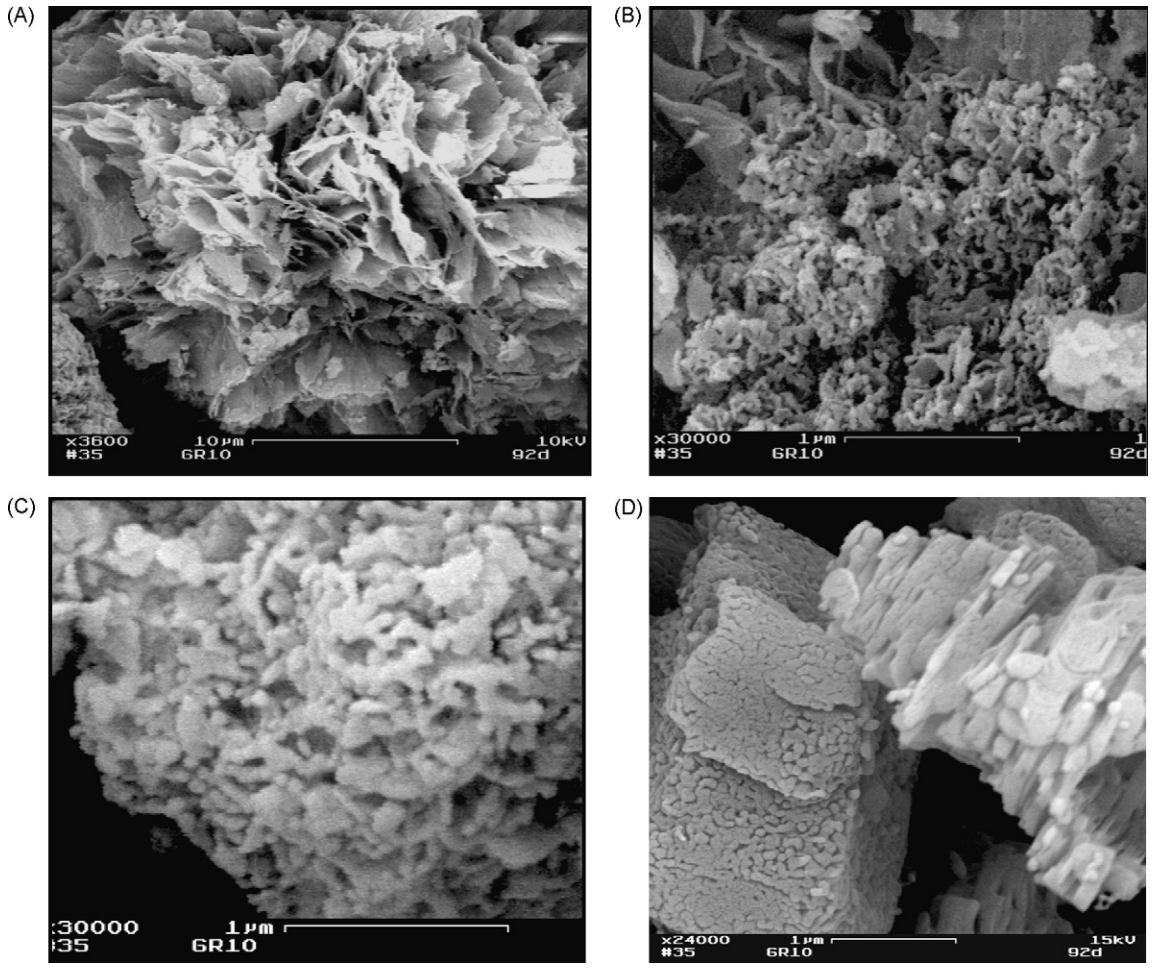

Fig. 1. SEM micrograph (A) aggregates of flake crystals of MgO, (B) an aggregate-like structure with small size similar to that of ortho-$Mg_3V_2O_8$ of Imp4Mg, (C) dense aggregate-like structure similar to that reported for pyro-$Mg_2V_2O_7$ of Imp5Mg, and (D) two different phases of pyro-$Mg_2V_2O_7$ and V_2O_5 of Imp6Mg.

groups on solid metal oxide support materials [24,27]. Accordingly, the relative amounts of surface hydroxyl groups of MgO and VO_x/MgO catalysts is similarly evaluated with TGA by recording the weight loss between 300 and 1000 °C (Table 1). The amount of deposited vanadium from the initial grafting process (Grf1Mg) after calcination matches closely the number of surface hydroxyl groups on the pure MgO surface as determined by this method. This indicates a near equimolar reaction of the surface hydroxyl groups with vanadyl trichloride (Scheme 1).

Additionally, the ratio of the secondary hydroxyl groups of this calcined catalyst (Grf1Mg) to vanadium ions is about 2, which is consistent with a stoichiometry as depicted in Scheme 1. By contrast, the amount of secondary hydroxyl groups on the non-calcined catalyst (Ungrf1Mg) is extremely high relative to the vanadium ion concentration. The ratio above 20 suggests that hydroxyl groups are not only detected at the surface but also from the inside of the $Mg(OH)_2$ lattice. Therefore, the TGA weight loss of 27.50 wt.% between 300 and 500 °C (Fig. 2) can be attributed to the transformation of $Mg(OH)_2$ to MgO. This agrees well with DTA results that show the conversion of $Mg(OH)_2$ to MgO as an endothermic peak at 430 °C and underlines the importance of calcinations in the preparation of such catalysts. The rather high dehydration temperature is in agreement with the literature where the dependence of the $Mg(OH)_2$ decomposition temperature on the preparation conditions and morphology of $Mg(OH)_2$ was established using TG, DTG and DTA techniques [34–38].

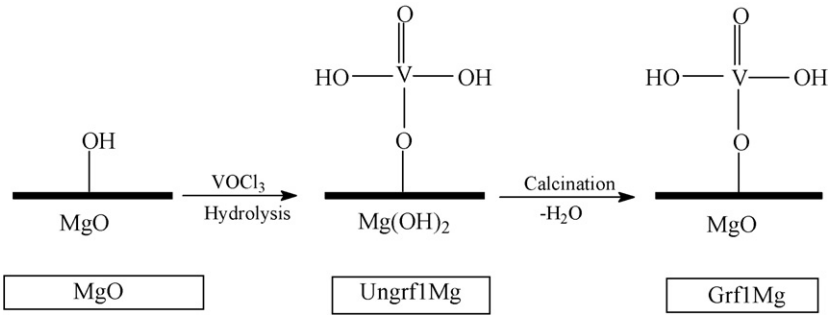

Scheme 1. Interconnection between the vanadylic species (V–OH) and unreacted OH groups of MgO followed by hydrolysis and calcination.

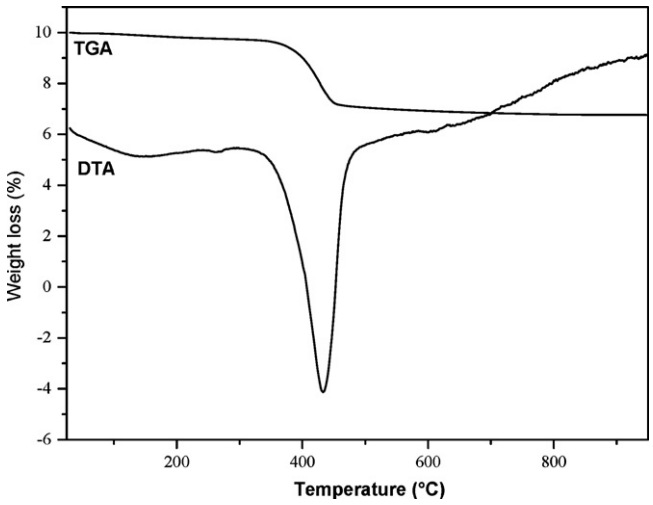

Fig. 2. Thermal analysis (TGA and DTA) of non-calcined grafted catalyst (Ungrf1Mg).

Repeating the grafting process reduces the concentration of hydroxyl groups below the number of vanadium ions in the second and third grafting process. This can be attributed to subsequent dehydration of vanadium hydroxide groups during calcinations leading to interconnection of vanadyl groups by V–O–V bonds [24].

3.1.2. Determination of surface area

For the calcined catalysts the BET surface areas and pore volumes decrease with increasing vanadium loadings but are generally higher than that of the bare MgO. The increase in surface area of the calcined catalysts relative to the bare support is likely to be a consequence of the hydration of the MgO surface layers occurring during the impregnation with the aqueous solution of ammonium metavanadate and the hydrolytic step during the grafting process. As reported before the contact with an aqueous medium results in a deep modification of the morphology of the MgO microcrystals. Extensive hydration to $Mg(OH)_2$ and subsequent dehydration to MgO account for the significant increase of the specific surface area [7].

This is nicely illustrated by comparison of the calcined and non-calcined grafted catalysts Grf1Mg and Ungrf1Mg, where calcination roughly triples the surface area. For the non-calcined grafted catalyst (Ungrf1Mg) the lowest surface area was determined which is actually below that of the bare support material.

3.1.3. Characterization with X-ray diffraction

The XRD patterns of the calcined grafted and impregnated VO_x/MgO catalysts with loadings 01.02–16.91 wt.% V display the characteristic reflexes of MgO at $2\theta = 42.75^\circ$, 62.10° and 36.90° [31,39]. By increasing the V loadings (Fig. 3), catalyst Imp4Mg (23.07 wt.% V) exhibits an additional sharp reflex at $2\theta = 35.15^\circ$ besides those characteristic of MgO. This suggests the existence of a significant amount of ortho-$Mg_3V_2O_8$ [39–41]. The catalyst Imp5Mg shows the typical reflexes related to pyro-$Mg_2V_2O_7$ (α-phase), besides the characteristic peaks of MgO [41,42]. Catalyst Imp6Mg with the highest loading (49.97 wt.% V) shows sharp reflexes related to pyro-$Mg_2V_2O_7$ and additional peaks at $2\theta = 15.30^\circ$, 20.25°, 21.60°, 26.05°, 30.90°, 32.30°, 34.35°, 41.20°, 45.45° and 51.20° revealing the presence of V_2O_5. The non-calcined catalyst (Ungrf1Mg) obtained from the initial grafting process, shows the characteristic pattern of $Mg(OH)_2$ the identity of which is further corroborated by thermal and spectroscopic measurements (DTA, TGA and IR).

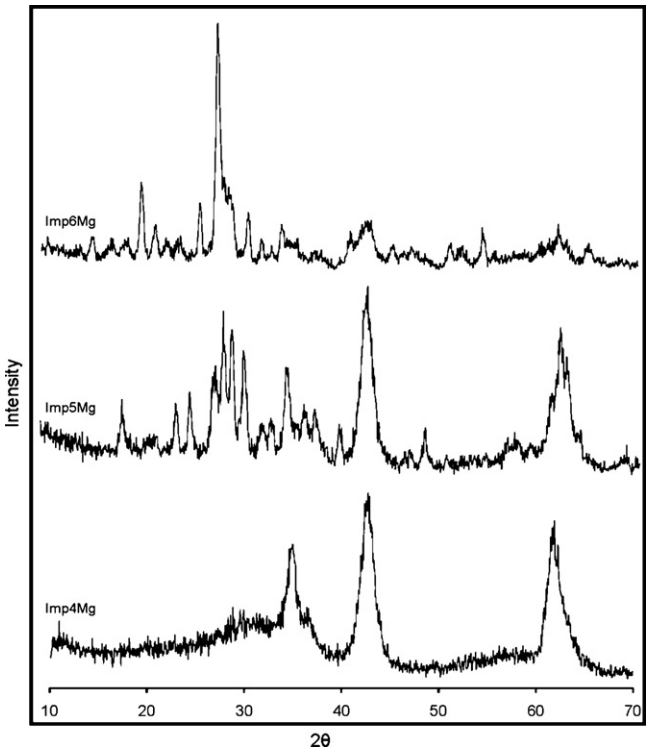

Fig. 3. XRD patterns of impregnated (VO_x/MgO) catalysts with high V loadings.

3.1.4. Characterization with IR spectroscopy

FT-IR spectra of the non-calcined catalyst obtained from the initial grafting process (Ungrf1Mg) show a strong band at 3694 cm^{-1} which can be assigned to the $\upsilon(OH)^-$ vibrational mode of the hydroxyl groups of the $Mg(OH)_2$ lattice (Fig. 4) [43,44]. This confirms the transformation of MgO to $Mg(OH)_2$ due to the hydrolytic step during the grafting process, which is in good agreement with the XRD data described before. The FT-IR spectra of the VO_x/MgO catalysts of 01.02–16.91 wt.% V prepared by grafting or impregnation are dominated by the characteristic features of MgO. By increasing the loading (Fig. 4), catalyst Imp4Mg shows bands at 816–860 and 640 cm^{-1}, which indicate the presence of ortho-$Mg_3V_2O_8$ species. Catalyst Imp5Mg shows the characteristic bands of pyro-$Mg_2V_2O_7$ at 966, 915, 836, 663, 675, 570 and 437 cm^{-1}. Finally, catalyst Imp6Mg with the highest loading shows a weak band at 1018 cm^{-1}, which can be attributed to the presence of V_2O_5. A strong band at 989 cm^{-1} with additional bands at 805–872, 687, 569 and 456 cm^{-1}, indicates the presence of pyro-$Mg_2V_2O_7$ (β-phase). ^{51}V solid-state NMR strongly supports this interpretation (see below). The bands around 3394 and 1619 cm^{-1} can be assigned to the stretching and bending modes of adsorbed water [44].

3.1.5. Characterization with UV–vis spectroscopy

The diffuse reflectance UV–visible spectra of VO_x/MgO catalysts either grafted or impregnated show absorption bands in the range of 200–445 nm, with a maximum at about 263 nm, which is typical for charge transfer transitions of V^{5+} ions in a monovanadate (VO_4) species [15–17]. Moreover, the impregnated catalyst (Imp6Mg) with the highest loading (49.97 wt.%) shows a broad band in the range of 200–425 nm with a shoulder at about 488 nm (Fig. 5). The broadening may indicate the presence of polymerized species of vanadium oxide, whereas, the additional shoulder refers to the existence of amorphous or crystalline V_2O_5 clusters [16]. The edge energy values have been used to characterize different VO_x containing compounds [17,20,21]. The E_g values obtained for the impregnated catalysts with vanadium loadings of 1.02–33.31 wt.%

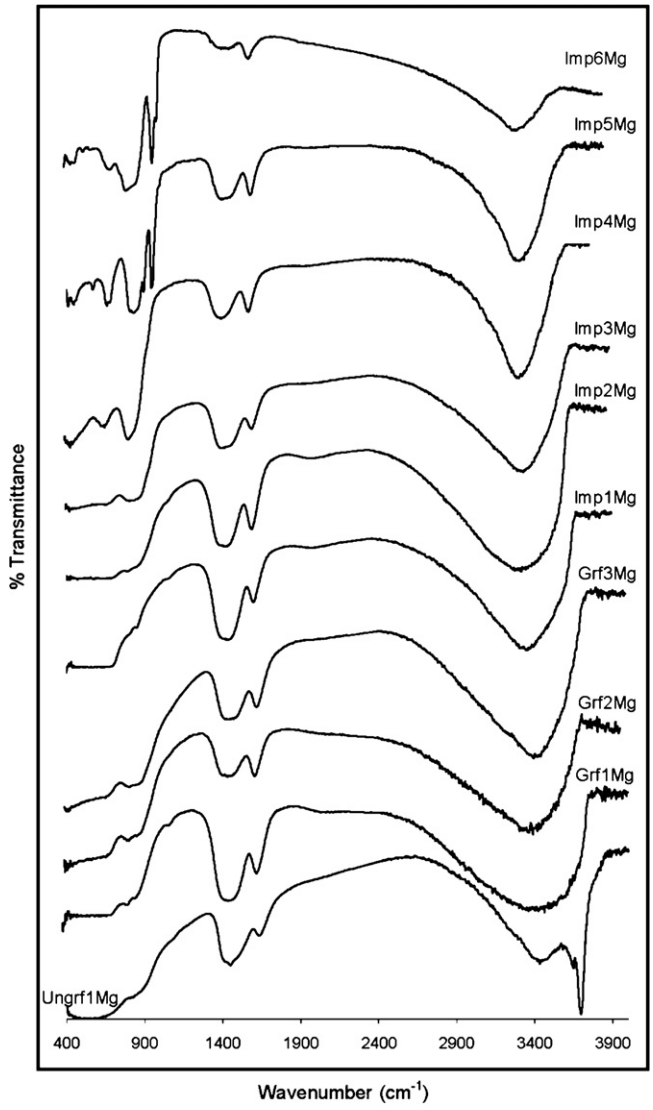

Fig. 4. FT-IR spectra of magnesia supported (VO_x/MgO) catalysts.

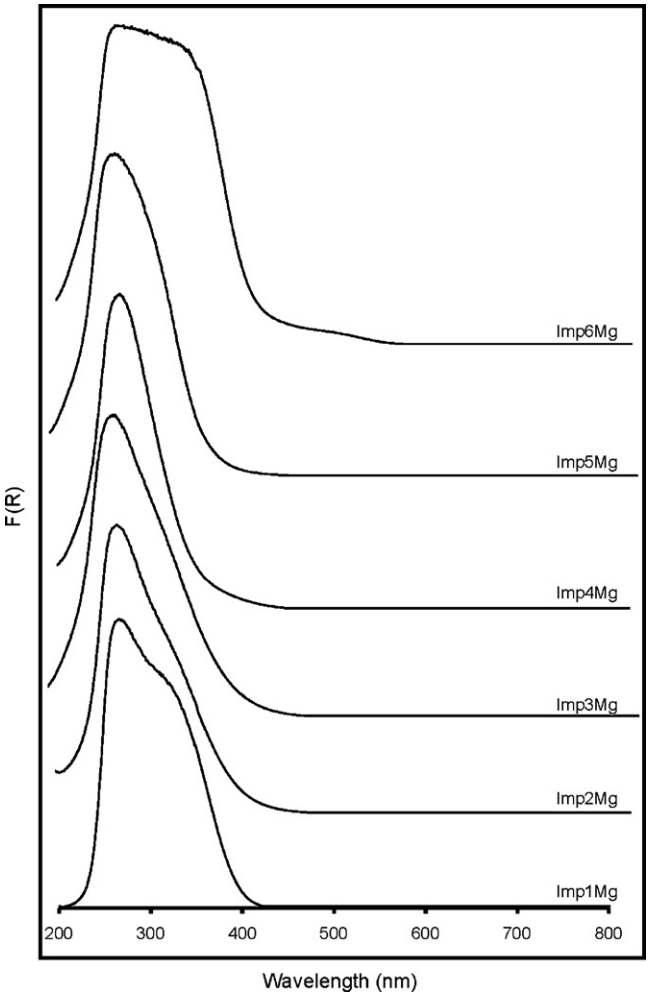

Fig. 5. DR–UV–visible spectra of impregnated (VO_x/MgO) catalysts.

are in the range of 3.62–3.52 eV, suggesting that the molecular structure of the surface vanadium oxide is quite similar, despite the variation of the vanadium loading. The proximity of the experimentally observed E_g values to that of ortho-$Mg_3V_2O_8$ implies that the structure of surface vanadium species in the present series of catalysts is essentially similar to that of ortho-$Mg_3V_2O_8$, which is composed of isolated VO_4 species [22,23]. However, the presence or absence of pyro-$Mg_2V_2O_7$ is still in ambiguous, since the E_g values for ortho-$Mg_3V_2O_8$ and pyro-$Mg_2V_2O_7$ phases are not so different. In contrast, the impregnated catalyst with the highest vanadium loadings exhibit an E_g value of 3.18, suggesting the presence of polymerized VO_5/VO_6 species besides isolated VO_4.

Table 2
Oxidation of cyclohexane using different VO_x/MgO and Mg–vanadates catalysts with the same surface area (0.02 m^2).[a].

Catalysts	%Conv.	TON	V conc. μ mol	$\%S_{Cy-OH}$	$\%S_{Cy=O}$	$\%S_{Cy-OOH}$	%(OS)	%By-prod.
Ungrf1Mg	22.31	24,877	00.23	20.29	31.71	42.96	94.96	01.12
Grf1Mg	04.77	6100	00.22	32.14	54.14	13.72	100.00	00.00
Grf3Mg	63.21	25,147	00.66	12.93	20.74	62.19	95.86	02.61
Imp1Mg	00.46	6333	00.02	44.35	55.43	00.00	99.78	00.01
Imp3Mg	40.14	22,017	00.49	09.59	16.88	71.33	97.80	00.88
Imp4Mg	63.13	12,180	01.36	10.87	13.75	70.54	95.16	03.05
Imp5Mg	67.13	13,030	01.31	13.06	16.67	62.42	92.15	05.26
Imp6Mg	65.22	5052	03.43	09.69	13.90	72.83	96.42	02.33
Ortho-$Mg_3V_2O_8$	63.91	311	53.59	06.70	12.14	75.77	94.61	03.44
Pyro-$Mg_2V_2O_7$	80.25	957	19.50	15.50	16.43	52.36	84.29	12.60
Meta-MgV_2O_6	75.25	197	90.01	25.40	20.54	39.47	85.41	10.97
Imp3Mg[b]	70.14	34,708	00.49	10.93	15.65	61.29	87.87	08.50

[a] Reaction conditions: cyclohexane (1.06 M, 27.56 mmol), H_2O_2 (0.4 M, 10.5 mmol), PCA (1.7×10^{-3} M, 0.044 mmol), CH_3CN (20 mL), 60 °C, 24 h. %By-products: 1,4-cyclohexanedione, 1,3-cyclohexanediol, 4-hydroxy-cyclohexanone, 2-hydroxy-cyclohexanone, 2,4-dihydroxy-cyclohexanone.
[b] The same reaction conditions a except H_2O_2 = 0.86 M, 22.36 mmol.

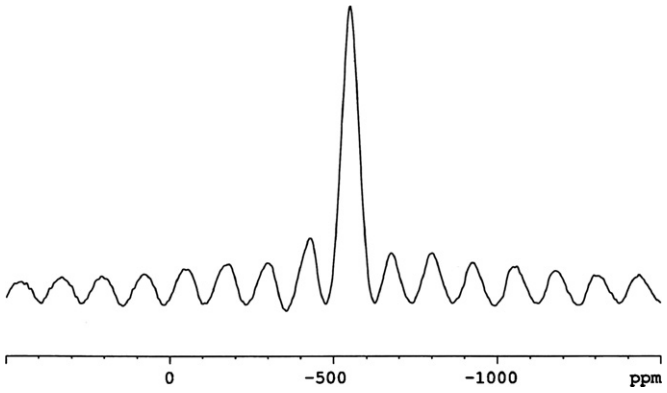

Fig. 6. ^{51}V MAS NMR spectrum of Imp3Mg at a spinning rate of 12.5 kHz.

3.1.6. *^{51}V solid-state NMR spectroscopy of VO_x/MgO catalysts*

Comparison of the ^{51}V NMR spectra of the catalysts with reference compounds of known structure provides information about the local environment of the vanadium sites, even for amorphous phases [31,45–49]. ^{51}V MAS NMR spectra of the VO_x/MgO catalysts with the best catalytic performance (Grf3Mg, Imp3Mg, Imp5Mg and Imp6Mg) have been recorded and compared to those obtained for ortho-$Mg_3V_2O_8$, pyro-$Mg_2V_2O_7$, meta-MgV_2O_6 and V_2O_5.

The impregnated catalyst (Imp3Mg) gives rise to a signal at −556 ppm and a side band pattern similar to that of ortho-$Mg_3V_2O_8$ (Fig. 6) [31,47,49]. The grafted catalyst obtained from the third grafting process (Grf3Mg) with the same vanadium loading as Imp3Mg catalyst shows a major signal at −556 ppm and an additional weak resonance at −431 ppm, the first signal indicates the presence of ortho-$Mg_3V_2O_8$. Both spectra (Figs. 6 and 7) are broader than those of the crystalline ortho-$Mg_3V_2O_8$, reflecting some disorder and/or small crystallite size [49]. The spectrum of the Imp5Mg catalyst (Fig. 8) shows the characteristic signals of pyro-$Mg_2V_2O_7$ (α-type). The narrow shape of these signals is quite similar to that of the pure pyro-$Mg_2V_2O_7$ (α-type), which confirms a comparable degree of structural order and crystal size [48]. The impregnated catalyst with high vanadium loading (Imp6Mg) gives a sharp resonance at −645 ppm and an additional small signal at −523 ppm. These two signals are due to V^{5+} in a highly distorted VO_4 environment as present in pyro-$Mg_2V_2O_7$ (β-type) [49]. Furthermore, the spectrum shows the characteristic signals of V_2O_5, indicating the presence of vanadium pentoxide (V_2O_5). An additional peak at −551 ppm suggests the existence of isolated VO_4 as that in ortho-$Mg_3V_2O_8$ (Fig. 9). Besides the information derived from chemical shift and line shape parameters like chemical shift anisotropy (CSA) and quadrupole interaction have been calculated from the spectra which are provided in the supplementary material including spectra of the reference materials.

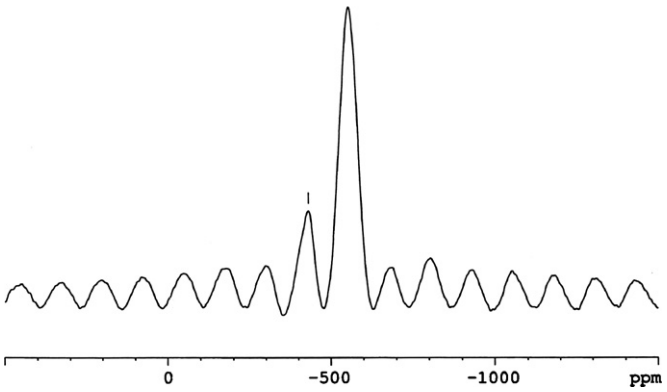

Fig. 7. ^{51}V MAS NMR spectrum of Grf3Mg at a spinning rate of 12.5 kHz.

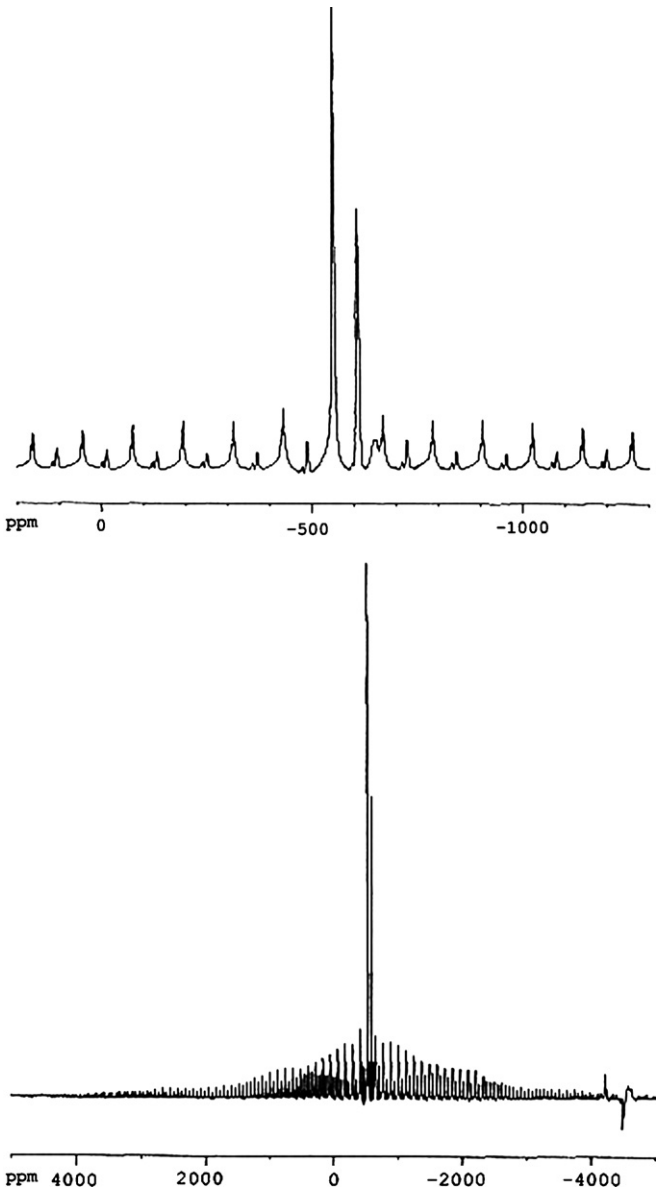

Fig. 8. ^{51}V MAS NMR spectrum of Imp5Mg at a spinning rate of 12.5 kHz.

3.2. *Catalytic activity*

According to the catalytic activity measurements, the main oxidation products of cyclohexane (Cy–H) are cyclohexylhydroperoxide (Cy–OOH) and to a minor extent a mixture of cyclohexanol (Cy–OH) and cyclohexanone (Cy=O). The latter can actually be considered as subsequent products derived from the primarily formed Cy–OOH via elimination of either H_2O or ½O_2. The optimum reaction conditions, high conversion, selectivity and TON, have been achieved by studying the effect of various parameters such as vanadium loading, vanadium distribution, catalyst amount, hydrogen peroxide concentration and reaction time.

The influence on conversion and TON have been studied by comparison of different (VO_x/MgO) catalysts at the same total vanadium concentration (11 μmol) (Fig. 10). The highest conversions are observed for catalysts with high vanadium loadings like Imp4Mg, Imp5Mg and Imp6Mg which contain phases such

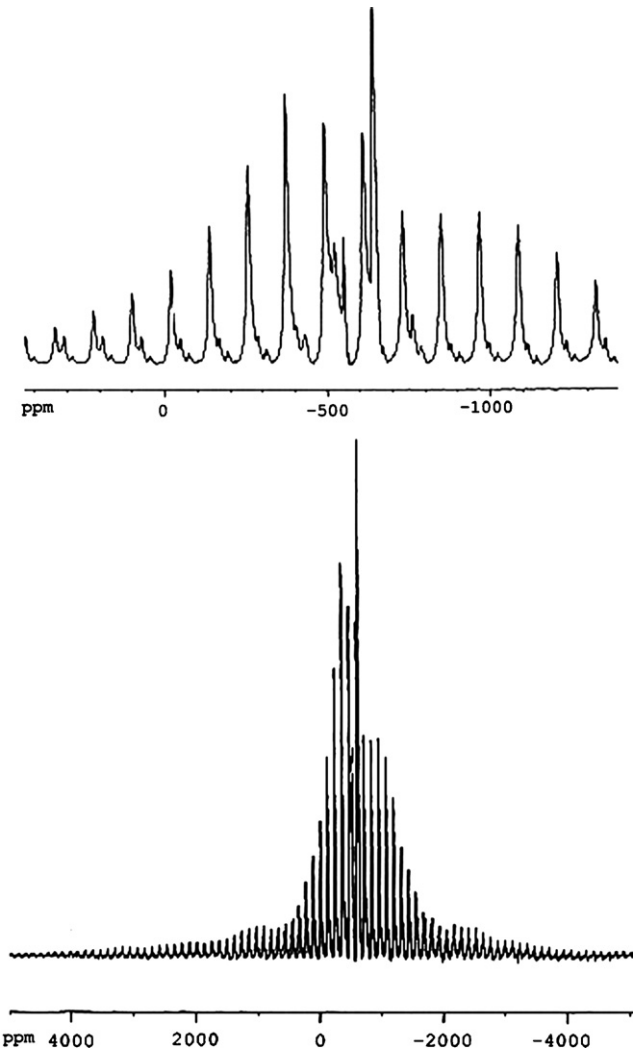

Fig. 9. ^{51}V MAS NMR spectrum of Imp6Mg at a spinning rate of 12.5 kHz.

as ortho-$Mg_3V_2O_8$ (Imp4Mg) and pyro-$Mg_2V_2O_7$ (Imp5Mg and Imp6Mg). In contrast, catalysts containing isolated VO_4 or merely minor amounts of ortho-$Mg_3V_2O_8$ such as in Imp1Mg, Imp2Mg and Imp3Mg do not show considerable conversion at this vanadium concentration. Moreover, the grafted catalysts which mainly contain isolated or highly dispersed ortho-$Mg_3V_2O_8$ such as Ungrf1Mg, Grf1Mg, Grf2Mg, and Grf3Mg at this vanadium concentration do not show significant conversion either. As it seems the homogeneously distributed vanadium species are in this case less active than the heterogeneously distributed ones with locally higher vanadium concentrations. A reason for the low activity of catalysts with low vanadium concentrations may be due to partial incorporation of vanadium into the bulk support. This is more significant at low vanadium concentrations and is corroborated by the discrepancy between the too low vanadium surface concentrations compared to the bulk concentrations as confirmed by EDX (Table 1) for these catalysts with low loadings. The reason for this incorporation of vanadium could be a consequence of the sheet-like morphology of MgO as detected by SEM. Alternatively, the low conversion rate for the catalysts with low loadings might be associated with a change in interaction of vanadium with the co-catalyst PCA. It is well known that V(V) forms complexes with PCA and peroxo ligands under comparable conditions [50,51]. Since the interaction of V(V) with PCA is actually crucial for the catalytic activity of this system [24], the reduced activity of highly diluted vanadium species might be a consequence of competitive complexation of PCA with Mg^{2+} ions. Actually, the presence of Mg^{2+}/PCA complex and H_2O accelerate the hydrolysis of acetonitrile to acetamide [52], which in fact could be identified by mass spectrometry. Moreover, PCA free V^{5+} species (uncomplexed V^{5+}) accelerate the decomposition of H_2O_2 to O_2 and H_2O which has a negative impact on the conversion rate as well. This latter effect was assessed by measuring the evolution of dioxygen from the decomposition of H_2O_2 via a volumetric apparatus similar to that described before [53]. In separate experiments no catalytic activity for H_2O_2 decomposition has been found for the plain MgO support or VO_x/MgO catalysts in presence of PCA under our reaction conditions. However, a slow decomposition of H_2O_2 is observed for all VO_x/MgO catalysts in the absence of PCA in the reaction medium.

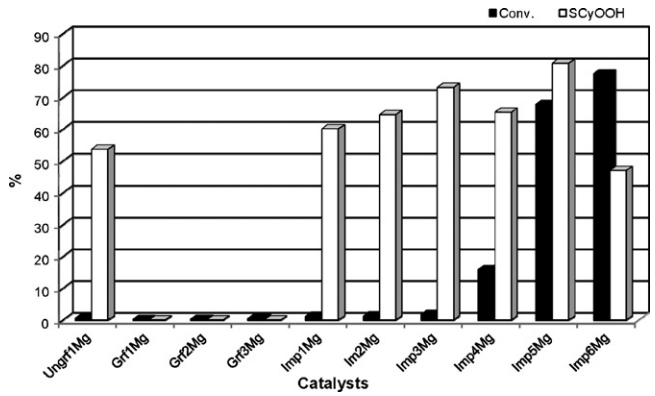

Fig. 10. Variation of conversion of cyclohexane and selectivity to cyclohexylhydroperoxide with different VO_x/MgO catalysts at equal V conc. (11 μmol).

The effect of the vanadium distribution on the catalytic activity was also studied for different VO_x/MgO catalysts at the same surface area (0.02 m^2) of Table 2. By applying the same surface area for impregnated or grafted VO_x/MgO catalysts a significant difference in cyclohexane conversion is noted. The increase in activity with increased vanadium loadings can be observed likewise for impregnated or grafted catalysts. The higher vanadium concentrations seem to be associated with the formation of more active phases such as ortho-$Mg_3V_2O_8$ and pyro-$Mg_2V_2O_7$ which then lead to an increase of conversion (see ESI). Also the bulk magnesium vanadates such as ortho-$Mg_3V_2O_8$, pyro-$Mg_2V_2O_7$ and meta-MgV_2O_6 give high conversion rates however with lower selectivities in comparison with catalysts like Grf3Mg, Imp3Mg, Imp4Mg, Imp5Mg and Imp6Mg containing ortho-$Mg_3V_2O_8$ or pyro-$Mg_2V_2O_7$ (see ESI). Generally, the impregnated catalysts show the best combination of high conversion and selectivity.

The effect of hydrogen peroxide concentration has been checked for an impregnated catalyst with an intermediate vanadium loading (Imp3Mg). By increasing the hydrogen peroxide concentration for Imp3Mg (Table 2), the conversion of cyclohexane is increased from 40.14 to 70.14% and the TONs value from 22,017 to 34,708. At the same time the selectivity to cyclohexylhydroperoxide drops from 71.33 to 61.29%. The higher concentration of H_2O_2 seems to accelerate the overoxidation of cyclohexylhydroperoxide to unwanted by-products. Therefore, the overall selectivity to the target products decreases from 97.80 to 87.87%.

Based on UV analysis, there is no significant leaching of vanadium from most of the grafted or impregnated catalysts prepared by us under the standard reaction conditions (Table 2). In contrast the impregnated catalyst with the highest vanadium loading (Imp6Mg) shows partial leaching (ca. 13%). This partial leaching corresponds to the presence of V_2O_5 at this high loading. From the literature is known that with increasing loading, the vanadium oxide struc-

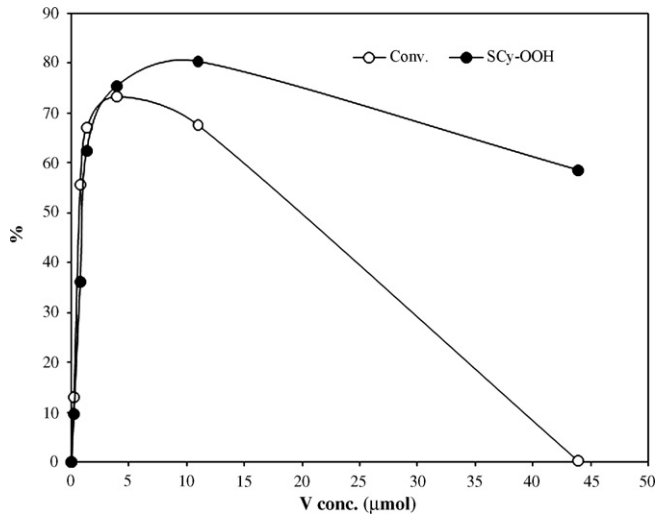

Fig. 11. Variation of cyclohexane conversion and selectivity to cyclohexylhydroperoxide with different amounts of catalyst Imp5Mg.

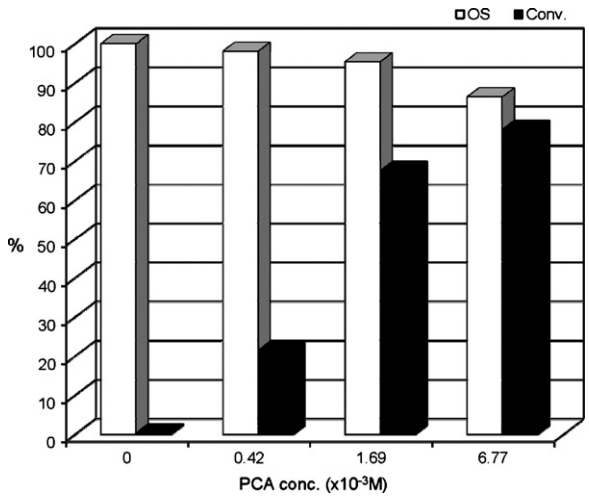

Fig. 12. Variation of cyclohexane conversion and overall selectivity (OS) of the target products with different conc. of PCA using catalyst Imp5Mg (11 μmolV).

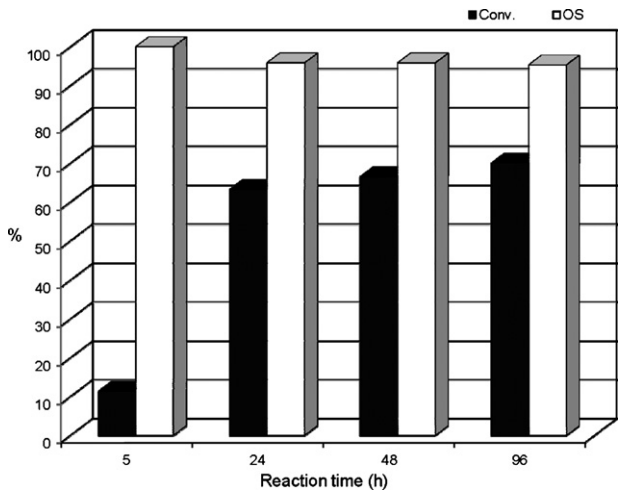

Fig. 13. Variation of cyclohexane conversion and overall selectivity (OS) of target products with reaction time (h), using catalyst Grf3Mg (0.66 μmolV).

ture changes gradually from monomer to polymer and finally to crystalline V_2O_5 [1,18].

In our case the identity of a fraction of V_2O_5 in Imp6Mg was confirmed by ^{51}V solid-state NMR, DRS and SEM. Generally the quite basic MgO support material seems to have a beneficial impact on the leaching rate compared to other support materials [24].

Different bulk magnesium vanadates and the better performing supported VO_x/MgO catalysts Grf3Mg, Imp3Mg, Imp4Mg and Imp5Mg have been tested for optimum reaction conditions. It can be noted that by increasing the amounts of ortho-$Mg_3V_2O_8$, pyro-$Mg_2V_2O_7$ and meta-MgV_2O_6 there is a considerable increase in cyclohexane conversion (see ESI). Similarly, increasing the amount of VO_x/MgO catalysts Grf3Mg, Imp3Mg, Imp4Mg and Imp5Mg also increases cyclohexane conversion (Fig. 11 and ESI). On the other hand, the conversion dramatically decreases at high concentrations of the supported catalysts (e.g., at 11 μmol of Imp3Mg). For the bulk magnesium vanadates the selectivity very soon decreases rapidly with increasing catalyst amount. The reduced conversion at high catalyst amounts can be explained by increased decomposition of H_2O_2 to O_2 and H_2O by PCA free V^{5+} species (uncomplexed V^{5+}). In order to confirm this conclusion, we decreased the relative amount of uncomplexed vanadium sites by increasing the concentration of PCA. We have chosen catalyst Imp5Mg to check this because it shows the highest conversion rate of our supported catalysts. As we found the catalytic activity (conversion) of Imp5Mg improves with increasing PCA concentration. However, raising the concentration of PCA increases not only the conversion of cyclohexane but decreases also the total selectivity of the target products (Fig. 12).

To check the effect of the contact time between catalyst and reaction mixture (i.e., reaction time) on conversion, product selectivity and TON, we varied this parameter for catalyst Grf3Mg which shows the highest TON of our supported catalysts in combination with one of the highest conversion rates. The results are summarized in Fig. 13 (and ESI), from which can be seen that the cyclohexane conversion and TON increase with the reaction time while the overall selectivity of the target products decreases only marginally. The lower selectivity at prolonged contact times can be explained by further oxidation of product which is of course more likely under these conditions. The increase of conversion rate and TON is however significant and roughly follows a saturation curve where the maximum (TON ca. 27,000) is reached after approximately 20 h for this specific sample. In conclusion, this result confirms well the high stability of the active sites at long reaction times.

4. Conclusions

In summary we prepared a series of VO_x/MgO catalysts via impregnation and grafting and investigated their structure and catalytic performance in the oxidative C–H activation of cyclohexane. According to XRD, IR and ^{51}V solid-state NMR measurements, impregnated and grafted catalysts with low loadings such as Imp1Mg, Imp2Mg, Grf1Mg and Grf2Mg do not contain any Mg-containing phases other than MgO. The presence of ortho-$Mg_3V_2O_8$ is observed for Imp3Mg and Grf3Mg. By increasing the vanadium loading, significant amounts of ortho-$Mg_3V_2O_8$ are found for Imp4Mg. Furthermore, significant amounts of pyro-$Mg_2V_2O_7$ can be detected for Imp5Mg, while Imp6Mg with the highest vanadium loading contains two different phases, pyro-$Mg_2V_2O_7$ and V_2O_5. The partial transformation of MgO to $Mg(OH)_2$ during the hydrolytic step of the grafting process was also confirmed by thermal and spectroscopic measurements (DTA, TGA, XRD and IR) for the uncalcined catalyst Ungrf1Mg.

According to our catalytic activity measurements, impregnated or grafted VO_x/MgO catalysts with low vanadium loading such as Imp1Mg, Imp2Mg, Ungrf1Mg, Grf1Mg and Grf2Mg containing isolated VO_4 species do not show considerable activity for the oxidation of cyclohexane. In contrary, the catalysts contain ortho-

$Mg_3V_2O_8$ and pyro-$Mg_2V_2O_7$ phases like Grf3Mg, Imp3Mg, Im4Mg, Imp5Mg and Imp6Mg show conversions ranging from 40 to 67% and TON values from 5052 to 25,147. Bulk magnesium vanadates such as ortho-$Mg_3V_2O_8$, pyro-$Mg_2V_2O_7$ and meta-MgV_2O_6 show activities similar to the supported catalysts containing these phases. Ortho-$Mg_3V_2O_8$ exhibits a higher activity than pyro-$Mg_2V_2O_7$, which in turn has a higher activity than meta-MgV_2O_6.

By increasing the amount of VO_x/MgO catalysts the cyclohexane conversion is increased as has been studied for Grf3Mg, Imp3Mg, Imp4Mg, Imp5Mg, and Imp6Mg. Beyond a maximum, the conversion however dramatically decreases at even higher catalyst concentrations, owing to a reduced interaction between PCA and active V(V) sites of the catalyst.

The stability against leaching, which can be a severe problem for oxide supported vanadium catalysts has been evaluated for our catalyst series using UV spectroscopy. For most catalysts either impregnated or grafted containing isolated VO_4 species do not show any significant leaching. The same is true for catalysts containing ortho-$Mg_3V_2O_8$, pyro-$Mg_2V_2O_7$ and meta-MgV_2O_6 which also do not show any leaching of vanadium. By contrast, catalyst Imp6Mg with the highest V loading shows partial leaching, which is attributed to the presence of V_2O_5 on the surface as confirmed by XRD, IR and SEM.

Acknowledgements

The authors would like to thank the Austrian Academic Exchange Service (ÖAD) for financial support for E.F.A. and the Austrian Science Fund (FWF) for funding (P17882-N11).

Appendix A. Supplementary data

Supplementary data associated with this article can be found, in the online version, at doi:10.1016/j.molcata.2009.11.007.

References

[1] A. Khodakov, B. Olthof, A.T. Bell, E. Iglesia, J. Catal. 181 (1999) 205–216.
[2] G. Deo, I.E. Wachs, J. Catal. 146 (1994) 323–333.
[3] X. Gao, J.L.G. Fierro, I.E. Wachs, Langmuir 15 (1999) 3169–3178.
[4] J. Haber, P. Nowak, E.M. Serwicka, I.E. Wachs, Bull. Pol. Acad. Sci. 48 (2000) 337–352.
[5] G.S. Wong, D.D. Kragten, J.M. Vohs, J. Phys. Chem. B 105 (2001) 1366–1373.
[6] M.A. Banares, Catal. Today 51 (1999) 319–348.
[7] G. Martra, F. Arena, S. Coluccia, F. Frusteri, A. Parmaliana, Catal. Today 63 (2000) 197–207.
[8] F. Arena, F. Frusteri, A. Parmaliana, Catal. Lett. 60 (1999) 59–63.
[9] J. Le Bars, A. Auroux, M. Forissier, J.C. Vedrine, J. Catal. 162 (1996) 250–259.
[10] K. Teramura, T. Tanaka, T. Yamamoto, T. Funabiki, J. Mol. Catal. A 165 (2001) 299–301.
[11] S.E. Dapurkar, A. Sakthivel, P. Selvam, J. Mol. Catal. A 223 (2004) 241–250.
[12] E.E. Wolf, Van Nostrand Reinhold, New York, 1992.
[13] E.G. Derouane, J. Haber, F. Lemos, F.R. Ribeiro, M. Guisnet, Nato ASI Series, Kluwer Academic Publishers, Dordrecht, The Netherlands, 1997.
[14] R.A. Periana, C&E News 79 (2001) 287–290.
[15] J.H. Lunsford, Catal. Today 63 (2000) 165–174.
[16] B.M. Weckhuysen, D.E. Keller, Catal. Today 78 (2003) 25–46.
[17] X. Gao, I.E. Wachs, J. Phys. Chem. B 104 (2000) 1261–1268.
[18] M.A. Vuurman, I.E. Wachs, J. Phys. Chem. B (1992) 5008–5016.
[19] P. Van Der Voort, M.G. White, M.B. Mitchell, A.A. Verberckmoes, E.F. Vansant, Spectrochim. Acta A 53 (1997) 2181–2187.
[20] D.E. Keller, T. Visser, F. Soulimani, D.C. Koningsberger, B.M. Weckhuysen, Vib. Spectrosc. 43 (2007) 140–151.
[21] B. Olthof, A. Khodakov, A.T. Bell, E. Iglesia, J. Phys. Chem. B 104 (2000) 1516–1528.
[22] G.C. Bond, S. Flamerz-Tahir, Appl. Catal. 71 (1991) 1–31.
[23] M. Ruitenbeek, A.J. van Dillen, F.M.F. de Groot, I.E. Wachs, J.W. Geus, D.C. Koningsberger, Top. Catal. 10 (2000) 241–254.
[24] E.F. Aboelfetoh, R. Pietschnig, Catal. Lett. 127 (2009) 83–94.
[25] D.E. Keller, D.C. Koningsberger, B.M. Weckhuysen, J. Phys. Chem. B 110 (2006) 14313–14325.
[26] D.E. Keller, F.M.F. de Groot, D.C. Koningsberger, B.M. Weckhuysen, J. Phys. Chem. B 109 (2005) 10223–10233.
[27] P. Wilson, P. Madhusudhan Rao, R.P. Viswanath, Thermochim. Acta 399 (2003) 109–120.
[28] G.B. Shul'pin, G.S. Mishra, L.S. Shul'pina, T.V. Strelkova, A.J.L. Pombeiro, Catal. Commun. 8 (2007) 1516–1520.
[29] Y.N. Kozlov, V.B. Romakh, A. Kitaygorodskiy, P. Buglyoĭ, G. Süss-Fink, G.B. Shul'pin, J. Phys. Chem. A 111 (2007) 7736–7752.
[30] V. Soenen, J.M. Hermann, J.C. Volta, J. Catal. 159 (1996) 410–417.
[31] D.S.H. Sam, V. Soenen, J.C. Volta, J. Catal. 123 (1990) 417–435.
[32] G.H. Jeffery, J. Bassett, J. Mendham, R.C. Denney, Vogel's Text Book of Quantitative Chemical Analysis, Longman, UK, 1989.
[33] D. Massiot, F. Fayon, M. Capron, I. King, S. Le Calvé, B. Alonso, J.O. Durand, B. Bujoli, Z. Gan, G. Hoatson, Magn. Reson. Chem. 40 (2002) 70–76.
[34] A. Corma, S. Iborra, Adv. Catal. 49 (2006) 239–302.
[35] E. Alvarado, L.M. Torres-Martinez, A.F. Fuentes, P. Quintana, Polyhedron 19 (2000) 2345–2351.
[36] W. Wang, X. Qiao, J. Chen, J. Am. Ceram. Soc. 91 (2008) 1697–1699.
[37] W. Wang, X. Qiao, J. Chen, H. Li, Mater. Lett. 61 (2007) 3218–3220.
[38] A. Corma, J.M. Lopez Nieto, N. Paredes, J. Catal. 144 (1993) 425–438.
[39] X. Gao, P. Ruiz, Q. Xin, X. Guo, B. Delmon, J. Catal. 148 (1994) 56–67.
[40] S. Sugiyama, Y. Iizuka, Y. Konishi, H. Hayashi, Bull. Chem. Soc. Jpn. 75 (2002) 181–186.
[41] S. Sugiyama, T. Hashimoto, N. Shigemoto, H. Hayashi, Catal. Lett. 89 (2003) 229–233.
[42] S. Sugiyama, Y. Iizuka, N. Fukuda, H. Hayashi, Catal. Lett. 73 (2001) 137–140.
[43] F. Freund, The Infrared of Minerals, Mineralogical Society, 1974.
[44] A. Corma, J.M. Lopez Nieto, N. Paredes, Appl. Catal. A: Gen. 104 (1993) 161–174.
[45] D. Rehder, in: J. Mason (Ed.), Multinuclear NMR, Plenum Press, New York, 1989.
[46] R.K. Harris, B.E. Mann, NMR and the Periodic Table, Academic Press, London, 1978.
[47] O.B. Lapina, V.M. Mastikhin, A.A. Shubin, V.N. Krasilnikov, K.I. Zamarev, Prog. NMR Spectrosc. 24 (1992) 457–525.
[48] M.L. Occelli, R.S. Maxwell, H. Eckert, J. Catal. 137 (1992) 36–50.
[49] T. Blasco, J.M. Lopez Nieto, Coll. Surf. A 115 (1996) 187–193.
[50] S. Pacigova, R. Gyepes, J. Tatiersky, M. Sivak, Dalton Trans. 1 (2008) 121–130.
[51] J. Tatiersky, P. Schwendt, M. Sivak, J. Marek, Dalton Trans. 13 (2005) 2305–2311.
[52] J. Gracia-Mora, D. Diaz, Transit. Met. Chem. 23 (1998) 57–61.
[53] J. Deren, J. Haber, A. Podgorecka, J. Burzyk, J. Catal. 2 (1963) 161–175.